Original article

In vitro and *in silico* evaluation of monoacylglycerol lipase inhibitory activity of apigenin carbamate derivatives

Tran The Huan[1,2*], Cao Thi Cam Nhung[1], Nguyen Thanh Bich Chau[1], Tran Thanh Dao[2]

[1]Faculty of Pharmacy, University of Medicine and Pharmacy, Hue University

[2]School of Pharmacy, University of Medicine and Pharmacy at Ho Chi Minh City

***Corresponding author:** Tran The Huan; Email: tthuan@hueuni.edu.vn

Received: 07/11/2025; **Accepted:** 15/01/2026; **Published:** 30/04/2026

DOI: 10.34071/jmp.2026.2.772

Abstract

Background: Monoacylglycerol lipase (MAGL) is a key enzyme in the endocannabinoid system, involved in multiple physiological and neurological processes. Developing MAGL inhibitors from semi-synthetic flavonoid scaffolds such as apigenin carbamates offers a promising approach.

Objectives: This study aimed to evaluate the MAGL inhibitory activity of semi-synthetic apigenin carbamate derivatives using integrated *in vitro* and *in silico* approaches.

Materials and Methods: Four apigenin carbamate derivatives synthesized from natural apigenin were tested for MAGL inhibition using a 4-nitrophenyl acetate hydrolysis assay. Binding affinity and complex stability were investigated through molecular docking and molecular dynamics simulations.

Results: Compounds A1 and A3 demonstrated improved MAGL inhibitory potency (IC_{50} 33.04 and 40.60 µM, respectively) over apigenin, with favorable predicted binding affinities and stable interactions in the enzyme active site. Molecular dynamics simulations indicated that A1 maintained greater conformational stability, whereas A3 formed more frequent hydrogen bond interactions.

Conclusion: Apigenin carbamate derivatives, particularly A1 and A3, are promising semi-synthetic leads for MAGL inhibitor development.

Keywords: *monoacylglycerol lipase, apigenin carbamate, enzyme inhibition, molecular docking, molecular dynamics.*

1. INTRODUCTION

Monoacylglycerol lipase (MAGL) is a membrane-associated serine hydrolase that catalyzes the hydrolysis of monoacylglycerols to glycerol and free fatty acids. Its principal endogenous substrate, 2-arachidonoylglycerol, is a key endocannabinoid involved in modulating pain perception, neuroinflammation, synaptic plasticity, and other central nervous system functions [1]. Pharmacological inhibition of MAGL elevates brain 2-arachidonoylglycerol levels and concomitantly reduces arachidonic acid-derived pro-inflammatory mediators, offering therapeutic potential in chronic pain, neurodegenerative diseases, and other central nervous system disorders [2]. However, achieving potency together with selectivity over related serine hydrolases remains a major challenge in MAGL inhibitor development [3].

Apigenin is a naturally occurring flavonoid widely distributed in plants such as celery, parsley, and chamomile [4]. It exhibits various biological activities, including antioxidant, anti-inflammatory, and neuroprotective effects [5]. Nevertheless, its relatively modest potency toward most protein targets and limited bioavailability have motivated structural modification strategies. From a structural perspective, apigenin is an attractive natural-product-derived scaffold due to its planar flavone core, suitable molecular size, and multiple phenolic hydroxyl groups, which allow efficient chemical derivatization while preserving favorable interaction potential within enzyme active sites. In our previous work, we designed and semi-synthesized a series of apigenin derivatives bearing carbamate moieties, which markedly enhanced inhibitory potency against acetylcholinesterase compared with the parent compound [6].

Notably, the carbamate functional group plays a central role in the inhibition mechanism of MAGL, as observed in the structures of selective MAGL inhibitors such as JZL-184 and ABX-1431 [7,8]. These compounds carbamoylate the catalytic serine within MAGL's active site, leading to sustained enzyme inactivation [9]. Given this mechanistic overlap, we hypothesized that our previously developed apigenin carbamate derivatives could also inhibit MAGL.

In this study, we evaluated the *in vitro* MAGL inhibitory activity of four apigenin carbamate derivatives and characterized their binding

interactions using molecular docking and molecular dynamics (MD) simulations. This integrated experimental–computational approach aims to assess the potential of carbamate-functionalized flavonoids as a versatile scaffold for the development of novel MAGL inhibitors.

2. MATERIALS AND METHODS

2.1. Compounds

The study investigated four apigenin carbamate derivatives (designated A1–A4), which were previously synthesized, purified, and structurally characterized by our research group [6]. All compounds were derived from the flavonoid apigenin and chemically modified through carbamoylation under basic conditions (K_2CO_3 in anhydrous acetone). The structural differences among the compounds primarily lie in the degree of hydroxyl substitution by carbamate moieties and the nature of the R substituent in the carbamate group (methyl or ethyl). The chemical structures and designations of these compounds are illustrated in Figure 1.

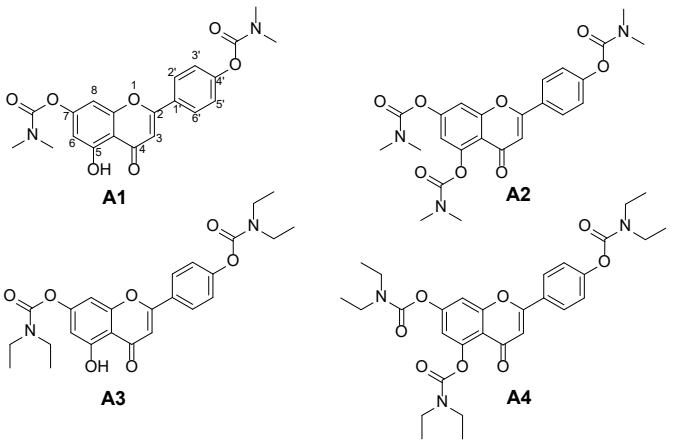

Figure 1. Chemical structures of apigenin carbamate derivatives A1–A4

2.2. *In vitro* MAGL inhibitory activity assay

MAGL inhibitory activity was measured following the method of Di Stefano et al. with modifications [10]. Briefly, assays were performed in 96-well plates (total volume 200 µL/well) at room temperature. Reaction buffer consisted of 10 mM Tris-HCl (pH 7.2), 1 mM EDTA, and 0.1 mg/mL bovine serum albumin (BSA). The substrate 4-nitrophenyl acetate (4-NPA; 100 µM final concentration) was freshly prepared in buffer. Test compounds (A1-A4) and the positive control JZL-184 were dissolved in DMSO and added to wells. Negative control wells received DMSO only. To initiate the reaction, 40 µL of recombinant human MAGL equivalent to 11 ng/well was added. Enzyme and inhibitor were pre-incubated for 10 min prior to substrate addition. Blanks without enzyme were included to correct for spontaneous hydrolysis of 4-NPA. After 30 min, absorbance at 405 nm was recorded using a Labomed EMR-500 plate reader. Each concentration was tested in triplicate in three independent experiments. IC_{50} values (µM) were calculated from concentration-response curves using a nonlinear regression model in GraphPad Prism (v8.4.3) [11].

2.3. Molecular docking study

Molecular docking was performed using AutoDock Vina version 1.1.2 to simulate the interactions between apigenin carbamate derivatives and the MAGL enzyme (PDB ID: 3PE6) [12,13]. The crystal structure of the enzyme was obtained from the Protein Data Bank and preprocessed using AutoDock Tools version 1.5.7 by removing water molecules and co-crystallized ligands, adding Kollman charges, polar hydrogens, and saving the structure in .pdbqt format [14].

The chemical structures of the apigenin carbamate derivatives were drawn using ChemDraw 16.0, converted into three-dimensional configurations, and energy-minimized using Open Babel version 3.1.1 [15]. The grid box was centered on the binding site of the co-crystallized ligand and configured to fully cover the enzyme's active site. Docking results included binding affinity values (kcal/mol) and binding poses, which were analyzed using Discovery Studio 2024.1 with a focus on key non-covalent interactions, including hydrogen bonding and hydrophobic contacts.

2.4. Molecular dynamics simulation

MD simulations were performed to evaluate the structural stability of the enzyme–ligand complexes under a simulated physiological environment and to elucidate the nature of persistent interactions

between the ligands and the active site of MAGL. Simulations were conducted using GROMACS version 2024.3 with the CHARMM36 force field applied for the protein [16,17]. Ligand parameters were generated using SwissParam [18].

The complexes showing the most promising inhibitory activity (based on *in vitro* and docking results), together with the MAGL apoprotein, were selected for MD simulations. The MD simulation protocol and parameter selection were adopted from our previously published work [19]. Each system was placed in a triclinic simulation box, solvated with TIP3P water molecules, and neutralized with Na^+ and Cl^- ions at a physiological salt concentration of 0.15 M. After energy minimization using the steepest descent algorithm, the system underwent equilibration in two phases: constant volume and temperature at 300 K, followed by constant pressure and temperature at 1 atm. Each equilibration phase lasted for 100 ps.

The production MD simulations were then performed for 100 ns with a time step of 2 fs, employing the leap-frog integrator and applying the LINCS algorithm to constrain bond lengths. Post-simulation analysis included calculation of the root mean square deviation (RMSD) to assess structural stability over time, root mean square fluctuation (RMSF) of amino acid residues, radius of gyration (Rg) to reflect protein compactness, solvent-accessible surface area (SASA), and the number of hydrogen bonds formed between the protein and the ligand throughout the simulation.

3. RESULTS

3.1. *In vitro* evaluation of MAGL inhibitory activity

The inhibitory activity of the four apigenin carbamate derivatives, along with the parent compound apigenin and the reference inhibitor, was evaluated *in vitro* based on IC_{50} values (Table 1). The results demonstrated that three of the four tested derivatives (A1, A2, and A3) exhibited notable inhibition against MAGL, with IC_{50} values ranging from 33.04 ± 1.02 µM to 124.47 ± 3.37 µM. In contrast, compound A4 showed no detectable inhibitory activity (IC_{50} > 200 µM).

Compared to the parent compound apigenin, derivatives A1 and A3 showed markedly enhanced biological activity, particularly A1, which achieved an IC_{50} value of 33.04 ± 1.02 µM. While the inhibitory potency of these carbamate derivatives remains lower than that of the positive control JZL-184, the findings confirm their potential to bind and partially inactivate the MAGL enzyme under the assay conditions.

Table 1. IC_{50} values of apigenin carbamate derivatives against MAGL

No.	Compound	IC_{50} ± SD (µM)
1	Apigenin	172.60 ± 7.05
2	A1	33.04 ± 1.02
3	A2	124.47 ± 3.37
4	A3	40.60 ± 1.64
5	A4	> 200
6	JZL-184	0.057 ± 0.003

3.2. Molecular docking results

The binding affinity of the apigenin carbamate derivatives to MAGL was assessed through molecular docking simulations. The results were evaluated based on predicted binding free energy (ΔG, kcal/mol) and non-covalent interactions at the active site. Table 2 summarizes the docking results, including ΔG values, hydrogen bonds, and key hydrophobic interactions between the ligands and amino acid residues within the catalytic pocket.

Table 2. Binding affinities of apigenin carbamate derivatives with MAGL (PDB ID: 3PE6)

Compound	ΔG (kcal/mol)	Hydrogen bonds	Hydrophobic interactions
Apigenin	-9.9	Ala51, Arg57	Ile179, Leu184, Tyr194, His269, Val270, Lys273
A1	-10.8	Ala51, Met123, Tyr194	Ile179, Tyr194, Leu205, Leu241, His269
A2	-9.8		Ala51, Ile179, Leu241
A3	-11.1	Ala51, Met123	Ile179, Leu205, Leu241, His269

A4	-8.9	Ser122, Ser176	Ala51, Ile179, Tyr194, Leu205, Leu241
JZL-184	-9.8	Ala51, Met123, Arg240	Leu213, Leu241

Among the compounds investigated, A3 exhibited the strongest predicted binding to MAGL with a ΔG of –11.1 kcal/mol, followed by A1 (–10.8 kcal/mol), both surpassing the reference inhibitor JZL-184 (–9.8 kcal/mol). Compounds A2 and A4 showed weaker predicted affinities, with ΔG values of –9.8 and –8.9 kcal/mol, respectively. The tested compounds also demonstrated a range of interactions with residues in the enzyme's active site, including both hydrogen bonds and hydrophobic contacts.

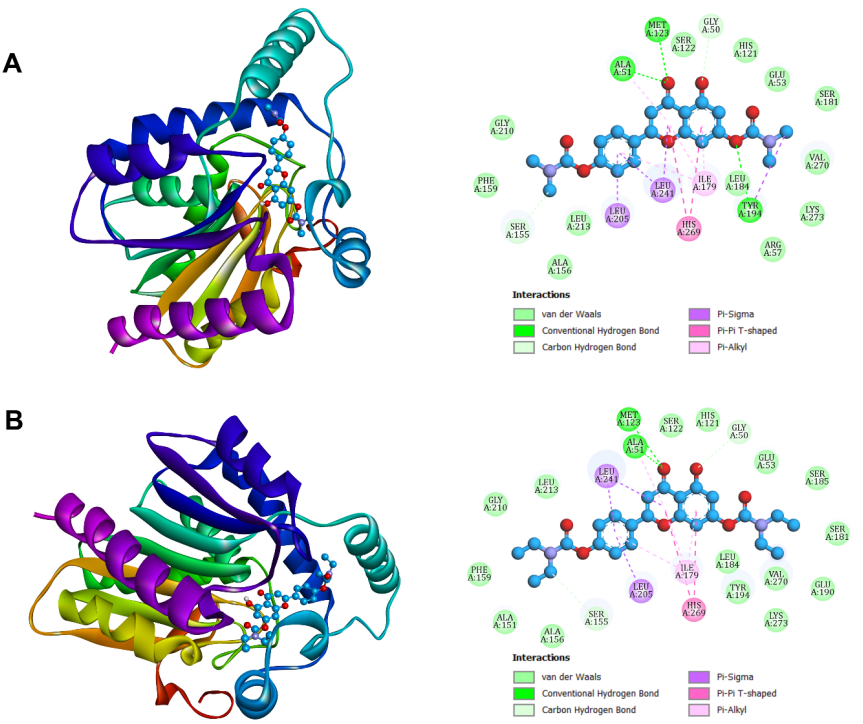

Figure 2. Three-dimensional and two-dimensional interaction diagrams between MAGL and ligand A1 (A), and ligand A3 (B)

Figure 2 shows the predicted binding poses and interaction maps of A1 and A3 in the MAGL active site. Both ligands occupied the catalytic pocket and formed hydrogen-bond interactions with Ala51 and Met123, together with hydrophobic contacts involving Ile179, Leu205, Leu241, and His269.

3.3. Molecular dynamics simulation results

Based on the *in vitro* MAGL inhibitory assay and molecular docking results, compounds A1 and A3, which showed the strongest inhibitory activities within the series, were selected for MD simulations together with the MAGL apoprotein to evaluate ligand-induced effects on enzyme stability. Dynamic parameters derived from 100 ns MD simulations of the MAGL apoprotein and ligand-bound systems are presented in Table 3. The MAGL apoprotein exhibited higher backbone RMSD values (0.200 ± 0.032 nm) compared to the ligand-bound systems, whereas both MAGL–A1 and MAGL–A3 complexes showed lower and comparable RMSD values (0.161 nm), indicating enhanced structural stability upon ligand binding. Similarly, the average C_α RMSF values of the complexes remained slightly lower than those of the apoprotein, suggesting reduced residue-level flexibility in the presence of ligands.

Differences were also observed in global compactness and solvent exposure. The MAGL apoprotein displayed higher radius of gyration and SASA values, while ligand binding resulted in reduced Rg and SASA, particularly for the MAGL–A1 complex, which exhibited the lowest values among the three systems.

Table 3. Average molecular dynamics parameters of MAGL apo, MAGL–A1, and MAGL–A3 systems over 100 ns

System	MAGL backbone RMSD (nm)	MAGL C_α RMSF (nm)	Rg of MAGL (nm)	SASA of MAGL (nm^2)	Ligand RMSD (nm)	Number of hydrogen bonds
MAGL apo	0.200 ± 0.032	0.103 ± 0.069	1.874 ± 0.014	139.987 ± 3.238	-	-
MAGL-A1	0.161 ± 0.033	0.099 ± 0.076	1.848 ± 0.008	135.183 ± 2.567	0.132 ± 0.035	1.928 ± 0.913
MAGL-A3	0.161 ± 0.023	0.095 ± 0.061	1.856 ± 0.009	139.304 ± 2.869	0.156 ± 0.059	2.112 ± 0.656

Regarding ligand stability, A1 displayed a lower average RMSD than A3, indicating a more stable binding conformation throughout the simulation. Conversely, A3 formed a higher average number of hydrogen bonds with the enzyme (2.112 bonds), implying stronger non-covalent interactions during the simulation period.

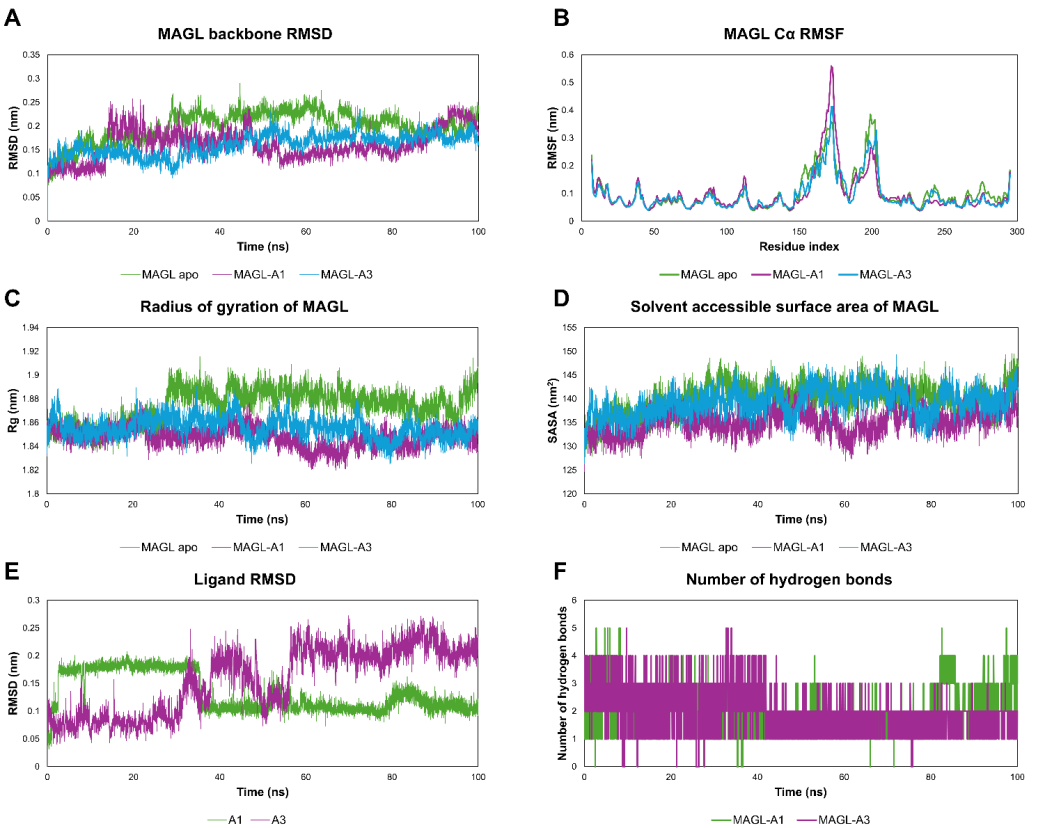

Figure 3. MD simulation analysis of MAGL apo, MAGL–A1, and MAGL–A3 systems over 100 ns.

Figure 3 presents the MD trajectories of the MAGL apoprotein and the MAGL–A1 and MAGL–A3 complexes over 100 ns. Both ligand-bound systems reached stable backbone RMSD values after approximately 15 ns, whereas the apoprotein exhibited higher overall fluctuations (Figure 3A). RMSF profiles remained low at the catalytic-site residues for all systems (Figure 3B). Compared to the apoprotein, ligand binding resulted in reduced Rg and SASA, with the MAGL–A1 complex showing the lowest values (Figure 3C–D). At the ligand level, A1 displayed lower RMSD values, while A3 formed a higher average number of hydrogen bonds during the simulation (Figure 3E–F).

4. DISCUSSION

4.1. *In vitro* inhibitory activity against MAGL

The *in vitro* biological evaluation revealed that A1 and A3 were the most promising compounds in terms of MAGL inhibition. From a structure–activity relationship perspective, both A1 and A3 were carbamoylated at only two hydroxyl groups (C_7 and

$C_{4'}$), while retaining a free hydroxyl group at the C_5 position. In contrast, A2 and A4 underwent complete carbamoylation, resulting in substitution at all three hydroxyl positions of the apigenin scaffold.

The superior activity of A1 and A3 suggests that the presence of a free hydroxyl group at C_5 may play a critical role in establishing hydrogen bonds with the enzyme, potentially contributing to more stable binding conformations and improved solubility in biological environments. This structure–activity trend is consistent with our recent studies on flavonoid carbamate derivatives based on other flavonoid scaffolds, including chrysin, luteolin, baicalein, and related compounds, where partial carbamoylation and retention of key hydroxyl functionalities were associated with enhanced enzyme inhibitory activity [11,19,20]. Together, these findings support the general applicability of the flavonoid–carbamate strategy and highlight the importance of controlled hydroxyl substitution for optimizing MAGL inhibition across different flavonoid frameworks.

4.2. Molecular docking analysis

The apigenin carbamate derivatives demonstrated favorable binding interactions with the MAGL enzyme based on molecular docking simulations. The observed hydrogen bonding and hydrophobic interactions of A1 and A3 with key active-site residues (Figure 2) suggest a favorable binding orientation that supports effective engagement of the MAGL catalytic pocket [21]. Both A1 and A3 retained the free hydroxyl group at the C_5 position of the apigenin scaffold, which may contribute to modulating ligand orientation and stabilizing interactions within the active site through indirect effects.

In contrast, A2 and A4 – both fully carbamoylated at all three hydroxyl positions – exhibited poor hydrogen bonding (A2) or weak interactions (A4), along with a reduced extent of hydrophobic contacts. This suggests that the absence of a free hydroxyl group negatively impacts the ligand's anchoring capability within the enzyme's binding pocket.

Interestingly, the parent compound apigenin, despite lacking a carbamate group, still displayed a relatively strong predicted binding affinity (–9.9 kcal/mol) and formed several notable interactions in the docking simulations. However, its low *in vitro* inhibitory activity highlights the role of the carbamate moiety in strengthening ligand–enzyme interactions and enhancing binding stability within the active site.

4.3. Molecular dynamics simulation analysis

The 100 ns MD simulations provided comprehensive insights into the structural stability and interaction characteristics of the MAGL enzyme in both its apoprotein form and in complex with the two ligands A1 and A3. Comparison with the MAGL apoprotein reveals that ligand binding plays a stabilizing role, as analysis of the protein backbone RMSD (Figure 3A) indicates that both MAGL–A1 and MAGL–A3 complexes maintained stable binding throughout the simulation with lower overall fluctuations than the apo enzyme, without inducing significant structural perturbation of the enzyme.

The RMSF profiles (Figure 3B) further suggest that ligand binding preserves the structural integrity of the catalytic site, as the key residues exhibited low fluctuation levels in both ligand-bound systems. In contrast, the apoprotein displayed higher flexibility in several regions, particularly outside the catalytic core. Minor variations were observed in flexible regions located at the N- and C-termini and in some non-functional loops, but these did not affect the catalytic core in any of the systems.

Differences in global compactness and conformational behavior were evident between the three systems. Relative to the apoprotein, both ligand-bound complexes adopted a more compact protein conformation, as reflected by reduced Rg values (Figure 3C). Among them, the MAGL–A1 complex showed a more compact and spatially stable protein conformation, as reflected by narrower Rg fluctuations. In contrast, binding of A3 was associated with increased structural flexibility, with broader Rg variations, particularly during the mid-stage of the simulation.

Similarly, SASA analysis (Figure 3D) indicates that the MAGL apoprotein exhibited the highest SASA, while ligand binding reduced surface exposure mainly in the MAGL–A1 complex. In contrast, the MAGL–A3 complex showed higher SASA values and larger fluctuations, comparable to those of the apoprotein, reflecting increased conformational adaptability.

At the ligand level, A1 maintained a more rigid and stable binding conformation, consistent with its lower average ligand RMSD (Figure 3E). In contrast, A3 exhibited higher conformational flexibility, although it stabilized after prolonged simulation time. Importantly, this increased flexibility of A3 was accompanied by the formation of a denser hydrogen-bonding network with the enzyme (Figure 3F), which may compensate for its dynamic behavior and contribute to sustained ligand–enzyme interactions.

In summary, comparison with the apoprotein highlights a ligand-induced stabilization of the MAGL structure, with A1 promoting superior

spatial and conformational stability, while A3 exhibits a more flexible binding mode supported by a denser hydrogen bonding network. Notably, these compounds have previously demonstrated enhanced acetylcholinesterase inhibitory activity relative to apigenin, underscoring the versatility of the flavonoid–carbamate scaffold for Alzheimer's disease–relevant targets [6]. Both compounds represent promising candidates for the development of MAGL inhibitors and warrant further structural optimization and biological evaluation, including studies on enzyme selectivity and *in vivo* relevance in neurodegenerative disease models.

5. CONCLUSION

This study evaluated the MAGL inhibitory activity of four apigenin carbamate derivatives using complementary *in vitro* and *in silico* approaches. Among the tested compounds, A1 and A3 demonstrated markedly improved inhibitory potency compared to the parent apigenin, as reflected by substantially lower IC_{50} values. Molecular docking suggested that both compounds engage in favorable non-covalent interactions with residues in the MAGL active site, while MD simulations over 100 ns provided further insight into their binding stability and dynamic behavior. A1 maintained greater conformational stability throughout the simulation, whereas A3 exhibited a denser hydrogen bonding network and higher structural flexibility within the binding pocket. Taken together, these results identify A1 and A3 as promising leads for further MAGL inhibitor development. The findings support the potential of chemically modified flavonoid scaffolds in early-stage drug discovery and provide a foundation for subsequent optimization, cellular assays, and *in vivo* pharmacological evaluation.

Acknowledgements

This research was financially supported by University of Medicine and Pharmacy, Hue University (Grant number: 16/25).

Authors declaration

The authors declare that there are no conflicts of interest regarding the research, authorship, or publication of this article.

REFERENCES

1. Deng H, Li W. Monoacylglycerol lipase inhibitors: modulators for lipid metabolism in cancer malignancy, neurological and metabolic disorders. Acta Pharm Sin B. 2020;10:582–602.

2. Choi S-H, Arai AL, Mou Y, Kang B, Yen CC-C, Hallenbeck J, et al. Neuroprotective Effects of MAGL (Monoacylglycerol Lipase) Inhibitors in Experimental Ischemic Stroke. Stroke. American Heart Association; 2018;49:718–26.

3. Deng H, Zhang Q, Lei Q, Yang N, Yang K, Jiang J, et al. Discovering monoacylglycerol lipase inhibitors by a combination of fluorogenic substrate assay and activity-based protein profiling. Front Pharmacol. 2022;13:941522.

4. Mushtaq Z, Sadeer NB, Hussain M, Mahwish, Alsagaby SA, Imran M, et al. Therapeutical properties of apigenin: a review on the experimental evidence and basic mechanisms. Int J Food Prop. Taylor & Francis; 2023;26:1914–39.

5. Salehi B, Venditti A, Sharifi-Rad M, Kręgiel D, Sharifi-Rad J, Durazzo A, et al. The Therapeutic Potential of Apigenin. Int J Mol Sci. 2019;20:1305.

6. The Huan T, Thi My Hanh N, Thai Son T, Thanh Dao T. Semi-synthesis of some carbamate derivatives of apigenin and evaluation of in vitro acetylcholinesterase inhibitory activity. Hue J Med Pharm. 2024;2024:95–100.

7. Lysenko LV, Kim J, Henry C, Tyrtyshnaia A, Kohnz RA, Madamba F, et al. Monoacylglycerol lipase inhibitor JZL184 improves behavior and neural properties in Ts65Dn mice, a model of down syndrome. PloS One. 2014;9:e114521.

8. Cisar JS, Weber OD, Clapper JR, Blankman JL, Henry CL, Simon GM, et al. Identification of ABX-1431, a Selective Inhibitor of Monoacylglycerol Lipase and Clinical Candidate for Treatment of Neurological Disorders. J Med Chem. American Chemical Society; 2018;61:9062–84.

9. Long JZ, Nomura DK, Cravatt BF. Characterization of monoacylglycerol lipase inhibition reveals differences in central and peripheral endocannabinoid metabolism. Chem Biol. 2009;16:744–53.

10. Di Stefano M, Masoni S, Bononi G, Poli G, Galati S, Gado F, et al. Design, synthesis, ADME and biological evaluation of benzylpiperidine and benzylpiperazine derivatives as novel reversible monoacylglycerol lipase (MAGL) inhibitors. Eur J Med Chem. 2024;263:115916.

11. Tran T-H, Tran T-S, Nguyen M-H, Pham T-T, Mai T-T, Tran T-D. Carbamoyl flavonoids as dual inhibitors of acetylcholinesterase and monoacylglycerol lipase: synthesis, in vitro evaluation, and computational studies. Med Chem Res. 2025;34:1544–56.

12. Trott O, Olson AJ. AutoDock Vina: improving the speed and accuracy of docking with a new scoring function, efficient optimization and multithreading. J Comput Chem. 2010;31:455–61.

13. Schalk-Hihi C, Schubert C, Alexander R, Bayoumy S, Clemente JC, Deckman I, et al. Crystal structure of a soluble form of human monoglyceride lipase in complex with an inhibitor at 1.35 Å resolution. Protein Sci. 2011;20:670-83.

14. Morris GM, Huey R, Lindstrom W, Sanner MF, Belew RK, Goodsell DS, et al. AutoDock4 and AutoDockTools4: Automated docking with selective receptor flexibility. J Comput Chem. 2009;30:2785–91.

15. O'Boyle NM, Banck M, James CA, Morley C, Vandermeersch T, Hutchison GR. Open Babel: An open chemical toolbox. J Cheminformatics. 2011;3:33.

16. Abraham MJ, Murtola T, Schulz R, Páll S, Smith

JC, Hess B, et al. GROMACS: High performance molecular simulations through multi-level parallelism from laptops to supercomputers. SoftwareX. 2015;1–2:19–25.

17. Croitoru A, Park S-J, Kumar A, Lee J, Im W, MacKerell AD, et al. Additive CHARMM36 Force Field for Nonstandard Amino Acids. J Chem Theory Comput. 2021;17:3554–70.

18. Bugnon M, Goullieux M, Röhrig UF, Perez MAS, Daina A, Michielin O, et al. SwissParam 2023: A Modern Web-Based Tool for Efficient Small Molecule Parametrization. J Chem Inf Model. American Chemical Society; 2023;63:6469–75.

19. Tran T-H, Doan D-N-H, Cao T-C-N, Tran T-S, Tran T-D. Flavonoid carbamate hybrids: design, synthesis, and evaluation as multi-target enzyme inhibitors for Alzheimer's disease. RSC Adv. The Royal Society of Chemistry; 2025;15:16855–68.

20. Tran T-H, Nguyen T-M-H, Cao T-C-N, Tran T-S, Mai T-T, Tran T-D. Integrating synthesis, enzyme inhibition and in silico studies: Carbamoyl luteolin derivatives targeting Alzheimer's disease. J Chin Chem Soc. 2025;72:739–50.

21. Scalvini L, Piomelli D, Mor M. Monoglyceride lipase: Structure and inhibitors. Chem Phys Lipids. 2016;197:13–24.